Cryogenically cooled 946nm Nd:YAG laser

S. J. Yoon* and J. I. Mackenzie

Optoelectronics Research Centre, University of Southampton, Highfield, Southampton SO17 1BJ, UK
**sjy1g12@orc.soton.ac.uk*

Abstract: We present the first multi-Watt demonstration of a diode pumped cryogenically cooled neodymium-doped yttrium aluminum garnet (YAG) laser operating at 946 nm on the $^4F_{3/2} \rightarrow {}^4I_{9/2}$ transition. 3.8 W of continuous wave output power for 12.8 W of absorbed pump was obtained with a slope efficiency of 47%. In addition, we made an extensive characterization of the spectroscopic properties around the pump and laser wavelengths over the temperature range of 77 K to 300 K to find an increase of ~2.5 times for both the absorption and emission cross sections at the lowest temperature.

OCIS codes: (140.3530) Lasers, neodymium; (140.3480) Lasers, diode-pumped; (140.3580) Lasers, solid-state; (010.1030) Absorption.

References and links

1. R. Zhou, E. B. Li, H. F. Li, P. Wang, and J. Q. Yao, "Continuous-wave, 15.2 W diode-end-pumped Nd:YAG laser operating at 946 nm," Opt. Lett. **31**(12), 1869–1871 (2006).
2. X. Délen, I. Martial, J. Didierjean, N. Aubry, D. Sangla, F. Balembois, and P. Georges, "34 W continuous wave Nd:YAG single crystal fiber laser emitting at 946 nm," Appl. Phys. B-Lasers Opt. **104**(1), 1–4 (2011).
3. S. P. Ng and J. I. Mackenzie, "Power and radiance scaling of a 946 nm Nd:YAG planar waveguide laser," Laser Phys. **22**(3), 494–498 (2012).
4. D. C. Brown, "The promise of cryogenic solid-state lasers," IEEE J. Sel. Top. Quantum Electron. **11**(3), 587–599 (2005).
5. T. Y. Fan, D. J. Ripin, R. L. Aggarwal, J. R. Ochoa, B. Chann, M. Tilleman, and J. Spitzberg, "Cryogenic Yb3+-doped solid-state lasers," IEEE J. Sel. Top. Quantum Electron. **13**(3), 448–459 (2007).
6. H. Glur, R. Lavi, and T. Graf, "Reduction of thermally induced lenses in Nd: YAG with low temperatures," IEEE J. Quantum Electron. **40**(5), 499–504 (2004).
7. D. C. Brown, "Ultrahigh-average-power diode-pumped Nd:YAG and Yb:YAG lasers," IEEE J. Quantum Electron. **33**(5), 861–873 (1997).
8. W. A. Clarkson and D. C. Hanna, "Resonator design considerations for efficient operation of solid-state lasers end-pumped by high-power diode-bars," in *Optical Resonator: Science and Engineering,* R. Kossowsky, M. Jelinek, J. Novak, eds. (Springer, Dordrecht, 1998).
9. W. P. Risk, "Modeling of longitudinally pumped solid-state lasers exhibiting reabsorption losses," J. Opt. Soc. Am. B **5**(7), 1412–1423 (1988).
10. T. Kushida, "Linewidths and thermal shifts of spectral lines in neodymium-doped yttrium aluminum garnet and calcium fluorophosphate," Phys. Rev. **185**(2), 500–508 (1969).
11. E. H. Carlson and G. H. Dieke, "The state of the Nd3+ ion as derived from the absorption and fluorescence spectra of NdCl3 and their Zeeman effects," J. Chem. Phys. **34**(5), 1602–1609 (1961).
12. B. Neuenschwander, R. Weber, and H. P. Weber, "Determination of the thermal lens in solid-state lasers with stable cavities," IEEE J. Quantum Electron. **31**(6), 1082–1087 (1995).
13. S. P. Ng and J. I. Mackenzie, "Planar waveguide laser optimization and characterization employing real-time beam quality measurement," IEEE J. Quantum Electron. **49**(2), 146–153 (2013).
14. N. P. Barnes, B. M. Walsh, R. L. Hutcheson, and R. W. Equall, "Pulsed F-4(3/2) to I-4(9/2) operation of Nd lasers," J. Opt. Soc. Am. B **16**(12), 2169–2177 (1999).
15. P. Hello, E. Durand, P. K. Fritschel, and C. N. Man, "Thermal effects in Nd-YAG-SLABS 3D modeling and comparison with experiments," J. Mod. Opt. **41**, 1371–1390 (1994).
16. R. L. Aggarwal, D. J. Ripin, J. R. Ochoa, and T. Y. Fan, "Measurement of thermo-optic properties of Y3Al5O12, Lu3Al5O12, YAIO(3), LiYF4, LiLuF4, BaY2F8, KGd(WO4)(2), and KY(WO4)(2) laser crystals in the 80-300 K temperature range," J. Appl. Phys. **98**(10), 103514 (2005).

1. Introduction

In recent years the output power and efficiency of the quasi-four-level Nd:YAG laser operating at 946nm has improved significantly [1–3]. Notwithstanding, there are three main

#204309 - $15.00 USD Received 7 Jan 2014; revised 31 Jan 2014; accepted 3 Feb 2014; published 31 Mar 2014

limitations for power scaling this laser system, firstly it's weak effective stimulated emission cross section, σ_e ~4 pm^2, secondly, the requirement for a high pump-intensity to reach threshold, in part due to reabsorption losses but also the low gain characteristics, which in turn implies a high thermal-load-density and results in significant thermo-optical aberrations, and third, strong competition with the higher-gain four level transition around 1.06 μm.

Cryogenic cooling has proven extremely beneficial for power-scaling ytterbium laser systems, capitalizing on the reduction in reabsorption losses, an increase in emission cross section, and more importantly, orders of magnitude improvement in the thermo-optical properties of the host media [4–6]. Despite this little effort has been devoted to neodymium-doped materials, presumably due to the larger quantum defect and therefore smaller extractable power and conversion efficiency, in addition to a higher heat load associated with the four-level 1.06 μm transition [7]. Nonetheless the potential for higher power operation of the quasi-four-level transition of Nd:YAG appears relatively unexplored, and quite rich, noting that two of the three limiting parameters for room-temperature operation will be drastically improved by cooling the active medium to cryogenic temperatures, namely increased gain and reduced quantum defect and hence thermo-optic degradation.

In this paper we have demonstrated for the first time, to the best knowledge, multi-Watt laser performance of the 946 nm $^4F_{3/2} \rightarrow {}^4I_{9/2}$ transition of Nd:YAG when cryogenically cooled in an optical-dewar. In these preliminary results, 3.8 W of output power was obtained with 12.8 W of absorbed pump leading to a slope efficiency of 47% under CW operation. In addition we studied in depth, the absorption characteristics of cooled Nd:YAG around the 800 nm pump wavelength to better understand the optimum pumping conditions. We observed an almost three-fold increase in the emission cross section, along with an equivalent reduction in the bandwidth of the strongest 808 nm absorption line.

2. Experimental setup

The Nd:YAG crystal and copper (Cu) mount were thermally isolated from the external environment via a vacuum insulated (<10^{-6} mBar) dewar cryostat. It is sealed with two 6 mm-thick windows, anti-reflection (AR) coated for wavelengths between 0.65 and 1.05 μm, providing optical access to the crystal from both.

To investigate the temperature dependence of the absorption cross section from the $^4I_{9/2}$ (Z) ground state to the $^4F_{5/2}$ and $^2H_{9/2}$ (S) Nd^{3+} excited states, we employed the configuration shown in Fig. 1. To obtain an optimum signal to noise ratio we used an AR coated 3 mm long 1at.% Nd:YAG rod wrapped in indium foil and held in contact with the cryogenically cooled Cu mount with a spring loaded clamp. Utilizing the broadband amplified spontaneous

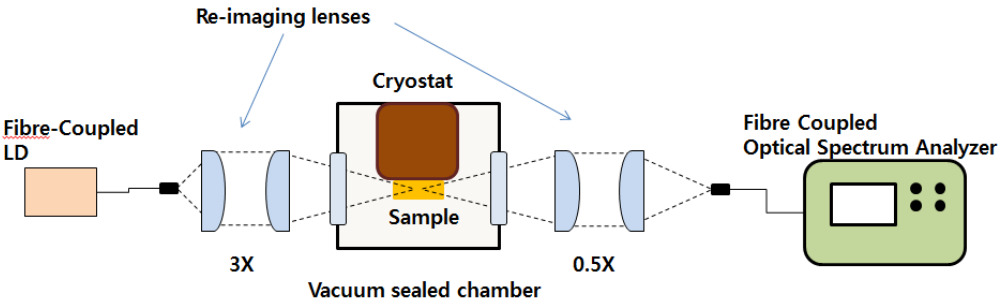

Fig. 1. Schematic of the experimental setup for the absorption spectra measurement.

emission (ASE) of a fiber-coupled diode laser (LIMO60-F200-DL808) just below its threshold current (<6.7 A), we could cover a wavelength range of ~40 nm about the main pump band of interest, i.e. 780 nm to 820 nm. With this setup we measured 10 mW of optical power exiting the Ø200 μm, NA 0.22 fiber core. A 3X telescope arrangement re-imaged the

#204309 - $15.00 USD Received 7 Jan 2014; revised 31 Jan 2014; accepted 3 Feb 2014; published 31 Mar 2014

fiber facet producing a 600 μm diameter focal spot in the crystal. Light passing through the sample was then re-imaged into a patch cord fiber (Ø300 μm NA 0.22) coupled to an optical spectrum analyzer (ANDO AQ6317B). The ASE spectrum was measured with and without the Nd:YAG crystal at a resolution of 0.1 nm and the absorption spectrum derived from the difference. In the calculations to determine the absorption cross section, the measured transmission data were corrected for the transmission of the optical coatings and set-up losses via the out of band transmission values and background measurements. Absorption spectra were recorded for crystal temperatures ranging from 296 K (RT) to 77 K (LNT).

For the laser experiment we used an uncoated 10 mm x 10 mm x 25 mm 1.0 at% Nd:YAG slab, oriented at Brewster's angle while "end-pumping" through one of the 10 mm x 25 mm faces (Fig. 2). The crystal was glued to a Cu mount bolted to the cold flange of the dewar, with an additional spring loaded clamping plate to ensure it did not detach. The transmission at the laser wavelength for the window AR coatings was measured to be ~99.5% each, effectively adding ~2% to the round trip cavity loss.

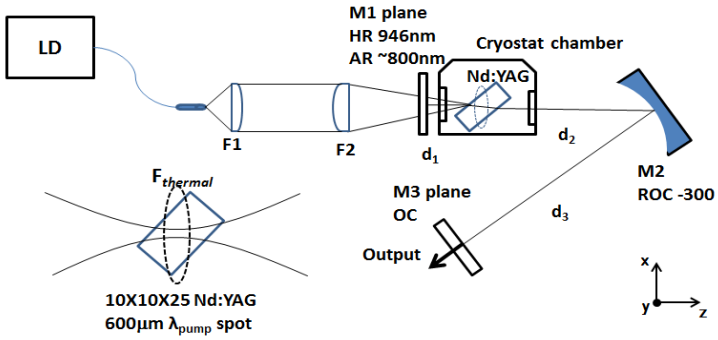

Fig. 2. Schematic diagram of the setup of the cryogenically cooled Nd:YAG laser.

The laser resonator was a three mirror V-cavity with the angle chosen to be as close as possible to that needed for reducing the astigmatism introduced by the Brewster angled slab [8], resulting in a nearly circular output beam. We report here results obtained with two different fiber-coupled diode laser pump sources, the first, providing a maximum of 25 W from a Ø400 μm core with 0.22 NA (JOLD-30-CPXF-1L), and the second, up to 60 W from a Ø200 μm core with 0.22 NA (LIMO60-F200-DL808). Both were operated with an emission peak around 808 nm. During the characterization phase of the cryogenic laser we operated the first diode (JOLD-30) in a QCW mode; driving it with 2 ms current pulses at a 4% duty cycle. As such we could explore the spectroscopic advantages of the decreasing crystal temperature without interference from pump-induced thermal loads. The aforementioned optical spectrum analyzer was used to check the lasing spectrum to ensure operation at 946 nm. Output power was measured using a Gentec thermopile power meter (UP19K).

Utilizing imaging telescopes, a minimum pump beam radius of ~300 μm was obtained approximately midway through the gain medium, corresponding to an average beam radius of ~390 μm (JOLD-30)/ ~327 μm (LIMO-60) over the crystal length. The coupling efficiency from the output of the pump delivery fiber into the crystal was 83%, including a measured reflection loss of ~10% for the un-polarized pump at the Brewster angled input surface. The absorption efficiency was ~84% at RT for the optimized wavelength for the JOLD-30 diode laser. With an effective thickness of 11.5 mm the crystal is significantly longer than would typically be used for optimal RT operation for the 946 nm laser transition. A plane pump-in-

#204309 - $15.00 USD Received 7 Jan 2014; revised 31 Jan 2014; accepted 3 Feb 2014; published 31 Mar 2014

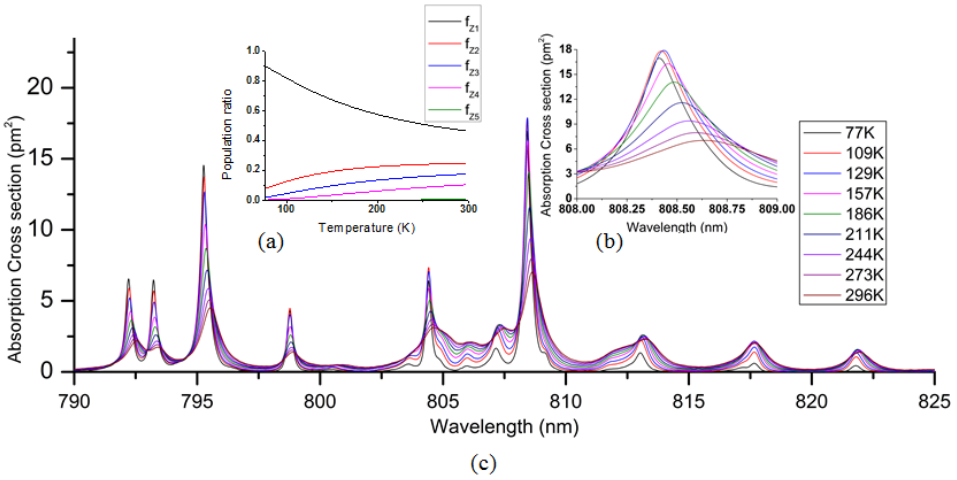

Fig. 3. (a) Stark levels Boltzmann population distribution for 4I9/2 (Z), (b) and (c) measured Nd:YAG (Z→S) absorption cross section at various temperatures between LNT and RT.

coupling high-reflectance (HR) mirror (M1) was positioned 65 mm in front of the laser crystal (d_1), while a turning mirror (M2) with a 300 mm radius of curvature (ROC) was positioned 240 mm behind the laser crystal (d_2). The final distance (d_3) between the 91.2%R plane output coupler (OC) and turning mirror M2 was set at 200 mm for QCW operation, and 165 mm for CW operation. All mirrors had a high transmission specification for 1.06 μm emission. At the lasing wavelength there was an additional <2% loss associated with the cavity mirrors and the Brewster angled gain medium, giving a total round trip cavity loss of ~3-4%. These configurations, as schematically shown in Fig. 2, produced a nominal cold cavity mode radius in the crystal of ~275 μm/~375 μm, for the respective d_3 values. The ratio of pump to laser beam size, $a = w_p/w_l$, following the notation from Risk [9], is between 1.4 and 1.5 (QCW) and 0.9-1.1 (CW), for a thermal lens focal length between infinity and 1m.

3. Results and discussion

Figure 3 shows the derived effective absorption cross section (σ_a^{eff}) spectra for Nd:YAG at various temperatures between RT and LNT. The neodymium concentration in the crystal was confirmed by comparing several other crystals of different lengths with the same specified doping level. At RT a maximum $\sigma_a^{eff} = 6.9 +/- 0.1$ pm^2 was observed at 808.7 +/– 0.1 nm. As expected from previous works [6, 10], a decreasing temperature increases the amplitude whilst reducing the bandwidth in equal measure, as shown in Fig. 4(b). However, a small deviation from this is observed at the lower temperatures, as the peak at 808nm increased to a maximum of $\sigma_a^{eff} = 18$ pm^2 around 120 K, then reduced to 16.9 +/– 0.2 pm^2 at 77K.

#204309 - $15.00 USD Received 7 Jan 2014; revised 31 Jan 2014; accepted 3 Feb 2014; published 31 Mar 2014

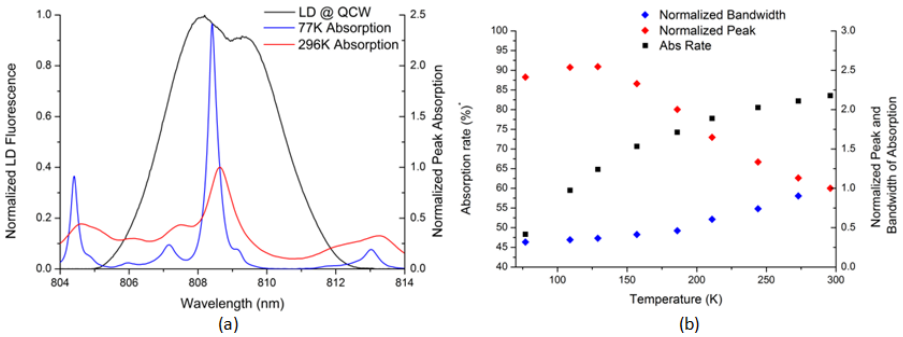

Fig. 4. QCW pump diode emission spectra at full current and RT normalized absorption cross sections for LNT and RT, (b): absorption efficiency vs crystal temperature (*calculated from measure spectra) and RT normalized peak and bandwidth of absorption.

This is attributed to the fact that this peak consists of two lines, $Z_1 \rightarrow S_1$ and $Z_3 \rightarrow S_4$, following the notation of [10, 11], and the fractional population in Z_3 starts to diminish quickly below 170K, while Z_1 is gaining over the same temperature range, nearly a 2-fold increase at LNT with respect to RT (Fig. 3(a)). The combined FWHM bandwidth decreased from ~1 nm at RT to 0.3 nm at LNT, and the peak wavelength blue-shifted by 0.2nm over this range, as shown in Fig. 3(b), in line with most other transitions as reported by Kushida [10].

The improved 946 nm laser performance investigated with QCW pumping clearly illustrates the significant spectroscopic advantages for this transition at cryogenic temperatures, independent of thermo optical effects, as shown in Fig. 5(a). With 2ms pulses at a 20Hz repetition rate, the maximum available average (peak) pump power was 1W (25W). Taking the measured spectrum of the diode laser pump we derived the pump absorption efficiency at different temperatures, assuming no ground state depletion. Figure 4(a) shows the measured QCW diode laser spectrum at its maximum operating power, compared with the absorption spectra (normalized to the RT peak). Despite the increase in peak absorption cross section at 808nm the actual pump-absorption efficiency reduced due to the narrowing linewidth, going from 84% at RT to 48% at LNT, as illustrated in Fig. 4(b).

At RT, laser threshold was reached at around the maximum available absorbed power, i.e. 700 mW, however at LNT it was only 114 mW leading to a slope efficiency of 63%. Despite having the highest slope at LNT, the maximum observed QCW output power was obtained with a crystal temperature at 176 K, 190 mW (4.25W peak) falling to 170 mW (4.75 W peak) at LNT, for the same incident pump power. Table 1 summarizes the laser performance at different crystal temperatures with respect to absorbed pump power. Beam quality was monitored using the method described in [12, 13] and at the maximum power was; M^2_x ~1.15, M^2_y ~1.25, with 4σ beam widths, w_x = 376 μm and w_y = 390 μm, at the output coupler.

While the 946 nm transition at RT is quasi-four-level with a degeneracy factor $\gamma = 1.012$ compared to $\gamma = 1$ for a true four level system and $\gamma = 2$ for a true three level system [14], the relatively long crystal length employed here had a comparatively large reabsorption loss. Using the B notation of Risk [9], being the ratio of the reabsorption to fixed cavity losses, we see (Table 1) that it ranged from 1.3 at RT to essentially zero at LNT. An increasing slope efficiency for the QCW laser with decreasing crystal temperature is a result of a combination of a modest value for S~10, for our configuration at the maximum output, a normalized parameter proportional to the intra-cavity laser power [9], and the gradually decreasing B value, as demonstrated by the dS/dF curves of reference [9]. The reducing threshold condition with lower temperatures is a combination of a diminishing Boltzmann occupation factor in Z_5 with an increasing population in R_1 and increasing emission cross section σ_e between these

#204309 - $15.00 USD Received 7 Jan 2014; revised 31 Jan 2014; accepted 3 Feb 2014; published 31 Mar 2014

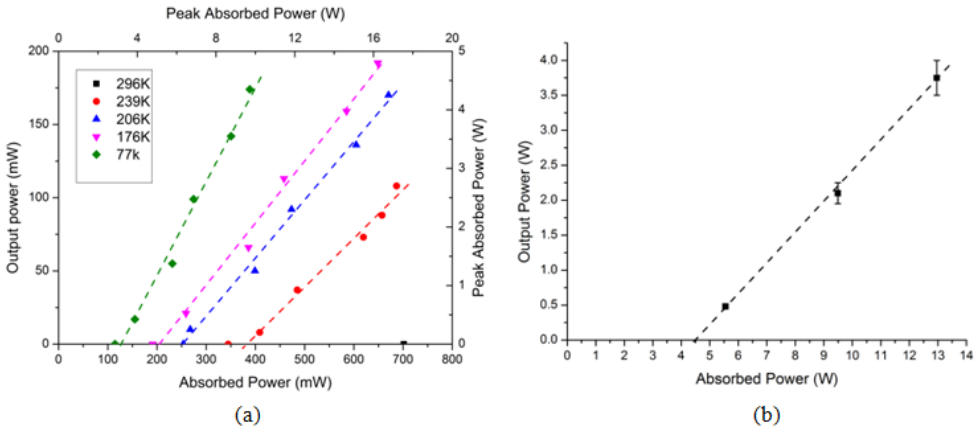

Fig. 5. QCW laser operation for LNT – RT, (b): CW laser operation at LNT.

Stark levels. The latter we determined via fluorescence measurements and the Füchtbauer–Ladenburg equation, at the various crystal temperatures of interest, the results of which are listed in Table 1.

Table 1. Threshold power, slope and optical-optical efficiency performance for QCW and CW modes of operation with respect to absorbed power, and the respective B-factors [9], Boltzmann occupation factors for the two Stark levels Z_5 and R_1, and our measured emission cross section between them, for temperatures between LNT and RT

	QCW (2ms pump pulse 4% duty cycle)					CW
Cu mount temp (K)	77	176	206	239	296	77
P_{th} (mW)	114	191	253	344	700	~4.5W
η_s (%)	63	42	40.7	31.5	-	47%
Optical to optical efficiency	45	30	25	16	-	29%
B [9]	$3x10^{-5}$	0.135	0.39	0.85	1.3	$3x10^{-5}$
f_{Z5}	$1x10^{-7}$	$6x10^{-4}$	$1.5x10^{-3}$	$3x10^{-3}$	$7.4x10^{-3}$	$1x10^{-7}$
f_{R1}	0.83	0.66	0.64	0.62	0.59	0.83
σ_e ($Z_5 \leftrightarrow R_1$) (pm^2)	10.9	9.7	9.3	8.7	6.6	10.9

In our non-optimum set-up for CW operation (LIMO60 pump source), and with the laser crystal cooled to LNT, we observed a maximum output power of 3.8 W for 12.8 W of absorbed pump power (25 W from the 200 μm fiber facet) leading to a slope efficiency of 47%, Fig. 5(b). Despite the expected thermo-optical advantages [6], and a cavity design should be stable with a thermal lens focal length as short as ~100 mm, we observed strong modal instability whilst trying to measure the M^2 in "real time" [12, 13], making it impossible to record a value. Using the approach of Hello et al. [15], it is evident that the ~2W thermal load at LNT can only produce a thermal lens focal length as short as 1m, assuming the thermo-optic properties of 2at.%Yb:YAG [16] (as this is the same host medium with a similar impurity level), but which can be >50% stronger in the x with respect to y-axis, depending upon the thermal interface impedance (R_{th}). Moreover if R_{th} between heat source and LN was high (>100 Kcm^2W^{-1}) it is possible for the crystal temperature to rise by >50K with a subsequent increase in the B factor and reduction in slope efficiency, however, this should not lead to the rapid modal switching we observed. One other source for cavity instability may have been the crystal mounting configuration along with the asymmetric crystal shape and cooling path, exacerbated by the Brewster angled facets, introducing astigmatic aberrations and perturbations favoring higher order modes. Currently we favor the last hypothesis, but need to investigate this further.

#204309 - $15.00 USD Received 7 Jan 2014; revised 31 Jan 2014; accepted 3 Feb 2014; published 31 Mar 2014

4. Conclusion

We have undertaken a preliminary study of the performance of a cryogenically cooled Nd:YAG 946 nm laser. Assessing the spectroscopic properties of the pump absorption band, in addition to the laser performance enhancement devoid of thermal effects, achieved by operating the laser in a low duty cycle QCW regime, we observed a better than 6-fold reduction in the absorbed threshold power and a maximum slope efficiency of 63% at LNT. As might be expected the potential laser performance for this transition is dramatically improved with respect to that obtainable at room temperature, where the laser would only just reach threshold, while at LNT we obtained 3.8 W output power for 12.8 W of absorbed pump leading to a slope efficiency of 47% under CW operation. Improved performance will be possible with line-narrowed diode pumping and an optimized geometry for thermal management of the gain medium.

Acknowledgments

S.J. Yoon would like to thank Charm Engineering Inc (Korea) for financial support via a PhD scholarship and J.I. Mackenzie support from EPSRC grants (EP/H005412/1; EP/J008052/1).

#204309 - $15.00 USD Received 7 Jan 2014; revised 31 Jan 2014; accepted 3 Feb 2014; published 31 Mar 2014